

Article

Optimum Design of Curved Surface Sliders Based on Site-Specific Seismic Input and Its Sensitivity

Felix Weber ^{1,*} , Leopold Meier ², Johann Distl ² and Christian Braun ³

¹ Maurer Switzerland GmbH, Neptunstrasse 25, 8032 Zurich, Switzerland

² MAURER ENGINEERING GmbH, Frankfurter Ring 193, 80807 Munich, Germany; L.Meier@maurer.eu (L.M.); J.Distl@maurer.eu (J.D.)

³ MAURER SE, Frankfurter Ring 193, 80807 Munich, Germany; C.Braun@maurer.eu

* Correspondence: F.Weber@maurer.eu; Tel.: +41-(0)44-520-8069

Received: 20 January 2018; Accepted: 22 February 2018; Published: 27 February 2018

Abstract: The design of curved surface sliders (CSS) based on the elastic response spectrum method with site-specific seismic input is commonly made by trial and error, whereby the design does not necessarily minimize structural acceleration. This paper therefore describes the optimum CSS design for minimum structural acceleration for given site-specific seismic input. All valid CSS designs and the optimum CSS design are represented by their associated trajectory in the elastic response spectrum plane that visualizes the optimization problem. The results demonstrate that the optimum CSS design is not obtained at maximum tolerated effective damping ratio. The subsequent sensitivity analysis describes how much the structural acceleration increases if the actual friction coefficient of the real CSS deviates from its optimum design value. The analysis points out that the increase in structural acceleration is approximately one order of magnitude smaller than the deviation in friction. The sensitivity data may be used by structural engineers to determine tolerable deviations in friction coefficient ensuring acceptable structural accelerations.

Keywords: curved surface slider; elastic response spectrum; friction; optimization; sensitivity

1. Introduction

Curved surface sliders (CSS) shift the natural period of the primary structure away from the time period range of high seismic energy and augment structural damping by friction damping [1]. For a selected isolation time period, the CSS may be designed by the elastic response spectrum method assuming friction coefficient and displacement capacity [2]. A valid CSS design is obtained if the maximum horizontal CSS force is equal to the maximum horizontal force of the primary structure due to the ground acceleration [2]. Thus, infinite CSS designs may be obtained by different combinations of friction coefficient and displacement capacity, but there is only one combination minimizing structural acceleration. This design freedom led to a variety of investigations on the damping in CSS. Back in 1991, Lai and Soong [3] started investigating the impact of CSS damping on structural acceleration, followed by Inaudi and Kelly [4] in 1993. Later the controversy discussion on the role of linearized CSS damping on CSS displacement capacity and structural acceleration was published in 1999 by Kelly [5] and Hall [6]. Du and Zhao [7] used a linearized two-degree-of-freedom model of the structure with CSS to investigate the optimum damping range of CSS. A first approach towards the optimization of the friction coefficient of CSS was presented by Jangid [8] in 2005 where the optimization criterion was to minimize both top floor acceleration and CSS relative motion for near-fault motion. Depending on the ground motion data the optimum friction coefficients turned out to be between 5% and 15%. Bucher [9] extended this optimization task by also taking into consideration the re-centring condition and Kovaleva et al. [10] further developed this approach to derive optimum CSS parameters for

various optimization functions. In the work of Nigdeli et al. [11], a linearized model of the structure with CSS was adopted to derive optimum CSS parameters that minimize structural acceleration with the constraint of a maximum tolerated CSS displacement capacity; a similar approach was used by Kamalzare et al. [12] to keep computational efforts within reasonable limits.

Common to most of the above mentioned studies is that basically optimum results only are shown but not all valid CSS design solutions. Also, the results of these studies are valid for certain ground motion data, but not for the entire possible variety of ground accelerations as specified by the elastic response spectra of type 1 and 2 with soil classes A, B, C, D, and E [2]. This paper tries to fill this gap by first showing the characteristics of all valid CSS designs from which the optimum CSS design for minimum structural acceleration directly follows. These computations are based on the common assumption that the isolated building may be modelled as a single degree-of-freedom system due to the design of the isolation time period; higher order modes and torsional effects are not considered [13]. In a next step it is shown how the characteristic variables, such as friction coefficient, displacement capacity, effective damping ratio, reduction factor, effective time period, and re-centring condition of all optimum CSS solutions depend on the selection of the isolation time period. These two first studies are performed for spectra of type 1 and 2 and soil class C. In the third and final section of the paper a sensitivity study is presented for all spectra types and soil classes, which describes by how much structural acceleration will deteriorate when the actual friction coefficient of the real CSS differs from its optimum value [14]. This study gives a clear statement on the acceptable tolerance of the friction coefficient of CSS and can be used by structural engineers to determine maximum tolerable deviations in the actual friction coefficient to still guarantee acceptably small structural accelerations.

2. Optimum Curved Surface Sliders for Minimum Structural Acceleration

Section 2.1 describes the CSS design adopting the linear elastic response spectrum method. The graphical representation of all the valid CSS designs in the response spectrum plane is shown and discussed in Section 2.2 based on which the optimum CSS design for minimum structural acceleration is obtained. The optimization results for spectra of type 1 and type 2 are given in Sections 2.3 and 2.4.

2.1. Linear Elastic Response Spectrum Method

The design parameters of the CSS are its isolation time period T_{iso} , which yields its effective radius R_{eff} of curvature, its friction coefficient μ that describes the dynamic friction coefficient between sliding material and sliding surface and its displacement capacity d_{bd} . The vertical load N_S on the CSS and the ground acceleration defined by the parameters of the linear response spectrum represent the input parameters to the CSS design.

The linear response spectrum describes the peak acceleration S_e normalized by the peak ground acceleration a_g as function of the time period T of the structure modelled as single degree-of-freedom (DOF) system whose damping ratio ζ_S is 5% (Figure 1) [2]. The standardized spectra of different earthquakes and soil classes are defined by their peak ground acceleration a_g , their type (1 or 2), their soil parameter S and the time periods T_B , T_C , and T_D . The type is related to the surface-wave magnitude and the parameters S , T_B , T_C , and T_D are related to the ground class. The numeric values of the parameters of the standardized spectra are given in [2]. The acceleration response at time periods $T_B \leq T < T_C$ is constant, at $T_C \leq T < T_D$ in proportion to T^{-1} , whereby its velocity is constant and at $T_C \leq T < T_D$ in proportion to T^{-2} , which results in constant displacement.

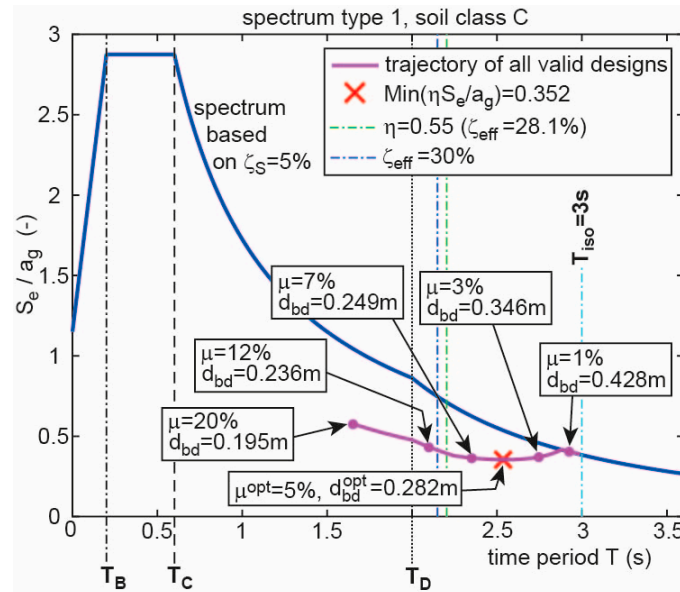


Figure 1. Elastic response spectrum including trajectory of all valid curved surface sliders (CSS) designs, limitations due to minimum reduction factor and maximum effective damping ratio and optimum CSS design for minimum structural acceleration. T : time period; T_B, T_C, T_D : time period ranges of response spectrum; T_{iso} : isolation time period; S_e : structural peak acceleration; a_g : peak ground acceleration; ζ_S : structural damping ratio; ζ_{eff} : effective damping ratio; η : reduction factor; μ : friction coefficient; μ^{opt} : friction coefficient of optimum solution; d_{bd} : displacement capacity; d_{bd}^{opt} : displacement capacity of optimum solution.

Once the response spectrum is defined by the soil dynamics experts the CSS design starts by the selection of the targeted isolation time period T_{iso} of the structure with CSS, which determines the effective radius R_{eff} of the curved surface of the CSS according to $R_{eff} = g(T_{iso}/2/\pi)^2$. Then, a combination of friction coefficient μ and displacement capacity d_{bd} of the CSS must be assumed in order to be able to compute the following states (Figure 2):

$$\text{Maximum horizontal CSS force : } F_b = \mu N_S + d_{bd} \frac{N_S}{R_{eff}} \tag{1}$$

$$\text{Effective stiffness: } k_{eff} = \frac{F_b}{d_{bd}} \text{ (not equal to restoring stiffness } N_S/R_{eff}) \tag{2}$$

$$\text{Effective time period: } T_{eff} = 2\pi \sqrt{\frac{N_S}{g k_{eff}}} \tag{3}$$

$$\text{Effective damping ratio: } \zeta_{eff} = \frac{2\mu}{\pi \left(\mu + \frac{d_{bd}}{R_{eff}} \right)} \text{ with constraint } \zeta_{eff} \leq 30\% \tag{4}$$

$$\text{Reduction factor: } \eta = \sqrt{\frac{0.10}{0.05 + \zeta_{eff}}} \text{ with constraints } 0.55 \leq \eta \leq 1 \tag{5}$$

$$\text{Reduced acceleration response of structure at effective time period : } \eta S_e(T = T_{eff}) \tag{6}$$

(acceleration response determined from spectrum and multiplied by η)

$$\text{Maximum horizontal force of structure(single DOF): } F_S = \eta S_e \frac{N_S}{g} \tag{7}$$

where $g = 9.81 \text{ m/s}^2$ is the gravitational field constant, ζ_{eff} must not be greater than 30% for linear calculation, the reduction factor η is limited to 1 if $\zeta_{\text{eff}} \leq \zeta_S = 5\%$, and $\eta \geq 0.55$ limits the reduction of the acceleration response of the structure if $\zeta_{\text{eff}} > 5\%$. Solving (5) for ζ_{eff} with $\eta = 0.55$ yields $\zeta_{\text{eff}} = 28.1\%$ (approx.), which shows that the minimum tolerated reduction factor $\eta = 0.55$ is triggered by ζ_{eff} being smaller than its maximum tolerated value of 30% for linear calculation.

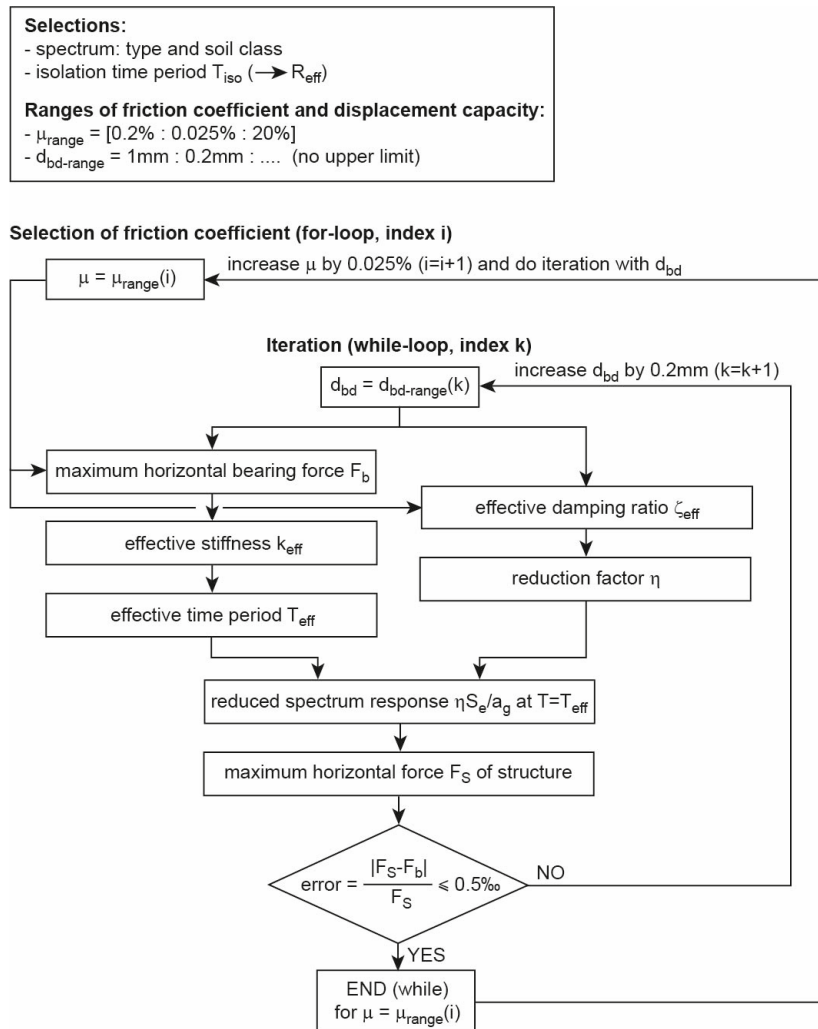


Figure 2. Flow chart of software program to compute all valid CSS designs. R_{eff} : effective radius; μ_{range} : range of friction coefficient; $d_{\text{bd-range}}$: range of displacement capacity.

A valid CSS design is obtained if the maximum horizontal force (1) of the CSS is equal to the maximum horizontal force (7) of the structure (with a reasonable error tolerance). If this condition is not fulfilled, the values assumed for μ and d_{bd} must be altered until $F_b \approx F_S$ is obtained. As the primary goal of this iterative procedure, which is commonly made by trial and error, is to satisfy $F_b \approx F_S$ the resulting CSS design—although a valid design—does not necessarily also minimize the acceleration response of the structural. The subsequent section therefore describes a procedure how to obtain all valid CSS designs due to all possible combinations of μ and d_{bd} based on which the CSS design leading to minimum structural acceleration can be identified.

2.2. Optimum CSS Design for Minimum Structural Acceleration

A software program is presented that allows computing any valid CSS design based on different combinations of μ and d_{bd} satisfying $F_b \approx F_S$; Figure 2 depicts the flow chart of this software program.

The software program basically consists of a for-loop where μ is selected based on the assumed friction coefficient range μ_{range} beginning at $\mu = 0.2\%$ and ending at $\mu = 20\%$ with an increment of 0.025% and a while-loop that computes d_{bd} for the selected μ such that the relative error of $F_b \approx F_S$ is not greater than 0.5% . For the assumed friction coefficient range with 792 elements this software program computes 792 valid CSS designs. These valid CSS designs are plotted in the spectrum plane in Figure 1 by their reduced normalized structural acceleration response $\eta S_e/a_g$ versus their effective time period T_{eff} . Due to the small increment in μ_{range} the plotted points of these valid CSS designs appear as a line, i.e., the trajectory of valid CSS designs. Along this trajectory the design parameters μ and d_{bd} of the valid CSS designs change, which is shown by some selected valid CSS designs with associated values of μ and d_{bd} . From this trajectory the following can be observed:

1. The trajectory of the valid CSS designs starts at $T_{eff} \approx T_{iso}$ due to the smallest considered friction coefficient $\mu = 0.2\%$ and then primarily propagates to the “left”, i.e., to lower values of T_{eff} due to the increasing values of μ and the acceleration response of the trajectory is reduced due to $0.55 \leq \eta \leq 1$.
2. As long as $\zeta_{eff} \leq 5\%$ the trajectory of the valid CSS designs is congruent with the non-reduced acceleration response of the spectrum because $\zeta_{eff} \leq \zeta_S = 5\%$ leads to $\eta = 1$.
3. For $5\% < \zeta_{eff} \leq 28.1\%$ the trajectory of the valid CSS designs is below the non-reduced acceleration response of the spectrum because $5\% < \zeta_{eff} \leq 28.1\%$ results in $0.55 \leq \eta < 1$.
4. To the “left” of the vertical dash-dotted line in green due to $\zeta_{eff} = 28.1\%$ and hence $\eta = 0.55$ the reduction factor remains at 0.55 despite ζ_{eff} increases up to its maximum tolerated value of 30% due to the increasing μ ; $\zeta_{eff} = 30\%$ is indicated by the blue vertical dash-dotted line.
5. There exists one optimum CSS design that is valid ($F_b \approx F_S$) and minimizes the structural acceleration response which is highlighted by the red cross on the trajectory.

The optimum CSS design is determined by the described software program after the computation of all the valid CSS designs from, which the pair of μ and d_{bd} is selected that minimizes the structural acceleration response. In the subsequent Sections 2.3 and 2.4 the optimum CSS designs are presented for spectra of type 1 and 2 and soil class C; the results due to other soil classes are omitted as their influence on the optimization results is little.

2.3. Optimization Results for Spectrum of Type 1 with Soil Class C

2.3.1. Optimum Solutions for Selected Isolation Time Periods

Four optimization trajectories due to four selected isolation time periods are presented. Figure 3a depicts the case of a rather unrealistically low isolation time period $T_{iso} = 1.9$ s, whereby the entire optimization trajectory lies in the region $T_C \leq T_{eff} < T_D$. The optimum CSS design is obtained at minimum tolerated $\eta = 0.55$ due to $\zeta_{eff} = 28.1\%$, i.e., on the green dash-dotted line. For the more realistic isolation time period $T_{iso} = 3.5$ s the main part of the optimization trajectory, including the optimum CSS design lies in the region $T_{eff} \geq T_D$ (Figure 3b). The optimum CSS design is characterized by $\zeta_{eff} = 17.8\%$ and $\eta = 0.662$. The optimization trajectory does not show how the state variables μ , d_{bd} , ζ_{eff} , η and T_{eff} change along the trajectory. Therefore, the state variables d_{bd} , ζ_{eff} , η and T_{eff} are plotted as function of the varied μ in Figures 4 and 5 for $T_{iso} = 1.9$ s and $T_{iso} = 3.5$ s. The force displacement loop of the optimum CSS solution is also included to demonstrate that the optimum CSS design fulfils the re-centring condition $E_s/E_h \geq 0.25$.

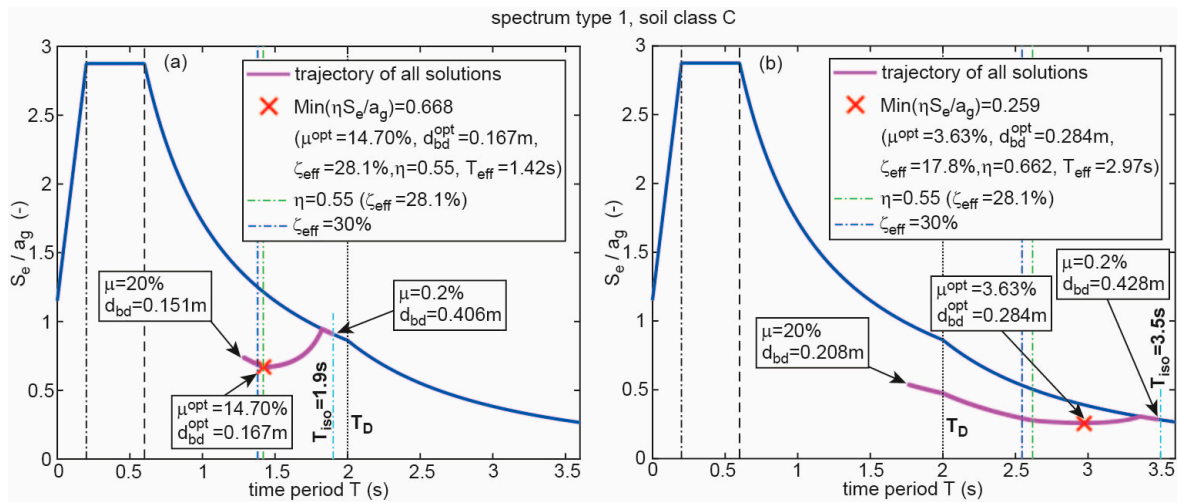


Figure 3. Optimization trajectories for (a) $T_{iso} = 1.9$ s and (b) $T_{iso} = 3.5$ s for spectrum type 1 with soil class C. T_{eff} : effective time period.

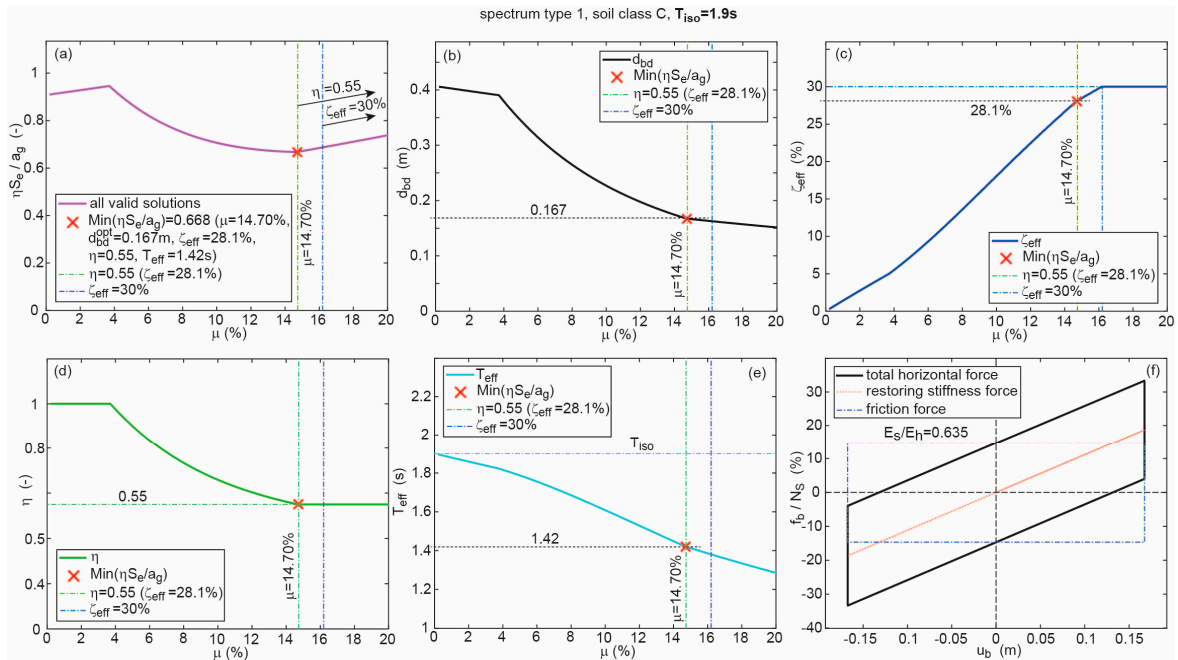


Figure 4. (a–e) Optimization results for $T_{iso} = 1.9$ s as function of friction coefficient and (f) force displacement curve of optimum CSS design for spectrum type 1 with soil class C. E_s : elastic energy; E_h : dissipated energy; u_b : isolator relative displacement.

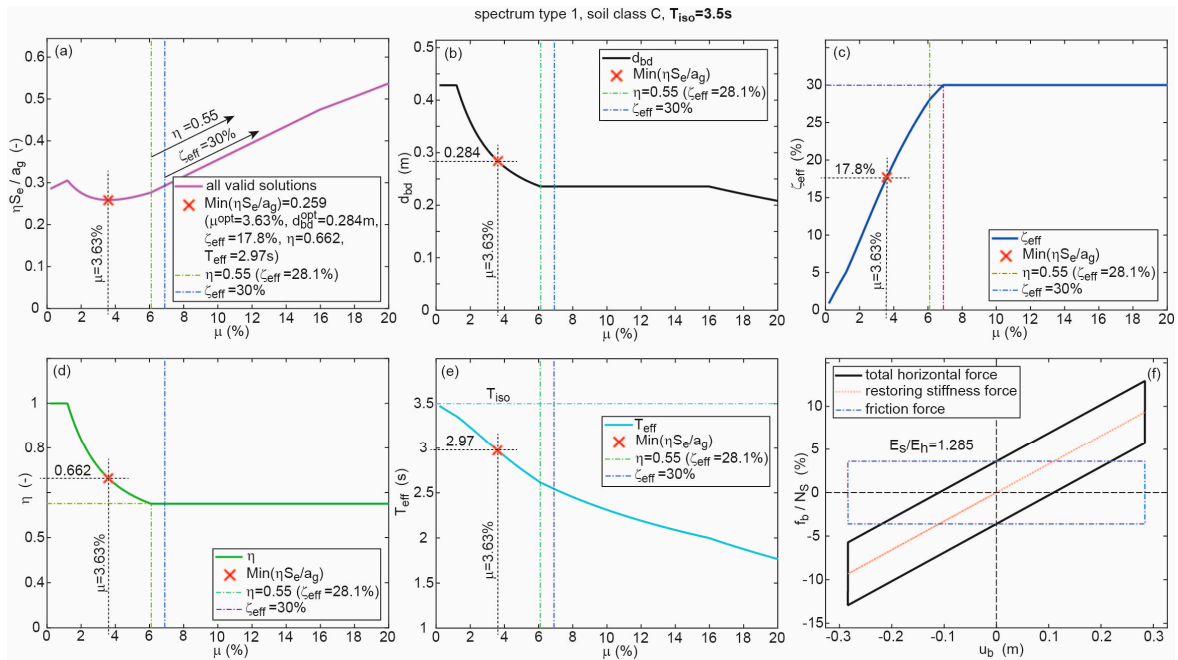


Figure 5. (a–e) Optimization results for $T_{iso} = 3.5$ s as function of friction coefficient and (f) force displacement curve of optimum CSS design for spectrum type 1 with soil class C.

The location of the optimum CSS design becomes nontrivial when the optimizations are performed for $T_{iso} = 2.49$ s (Figure 6) and $T_{iso} = 2.50$ s (Figure 7). For $T_{iso} = 2.49$ s the optimum CSS design lies in the region $T_{eff} < T_D$, because the optimization trajectory, which shows a first local minimum at $T_{eff} > T_D$ in Section (ii), drops again in Section (iii) generating the global minimum at $T_{eff} < T_D$ (Figure 6b). The optimum CSS design is characterized by $\zeta_{eff} = 28.1\%$ and $\eta = 0.55$. In contrast, if $T_{iso} = 2.50$ s is selected the global minimum is obtained at $T_{eff} > T_D$ with $\zeta_{eff} = 17.8\%$ and $\eta = 0.662$ similar to the results obtained for $T_{iso} = 3.50$ s (Figure 7b).

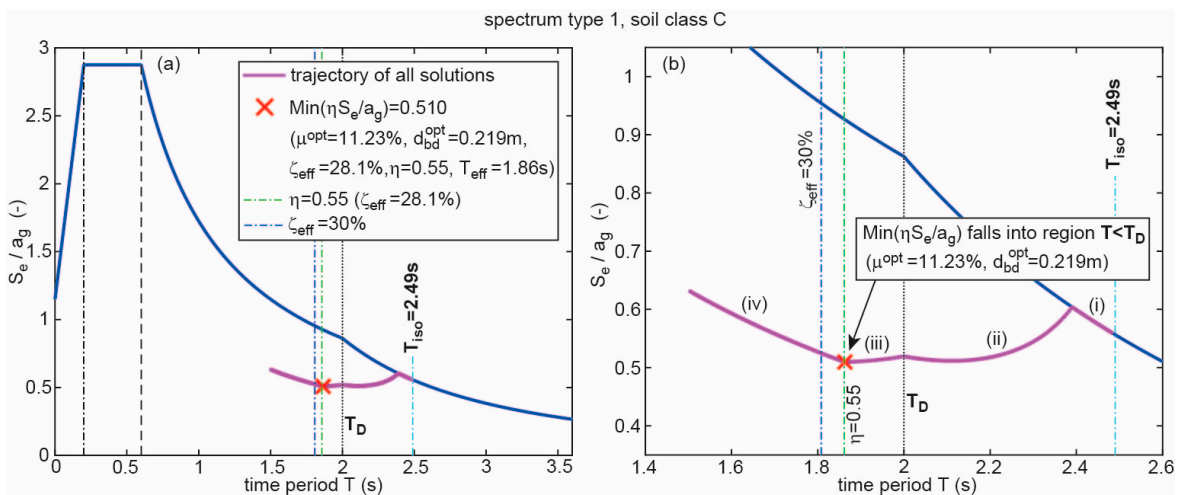


Figure 6. (a) Optimization trajectory for $T_{iso} = 2.49$ s and (b) according close-up for spectrum type 1 with soil class C.

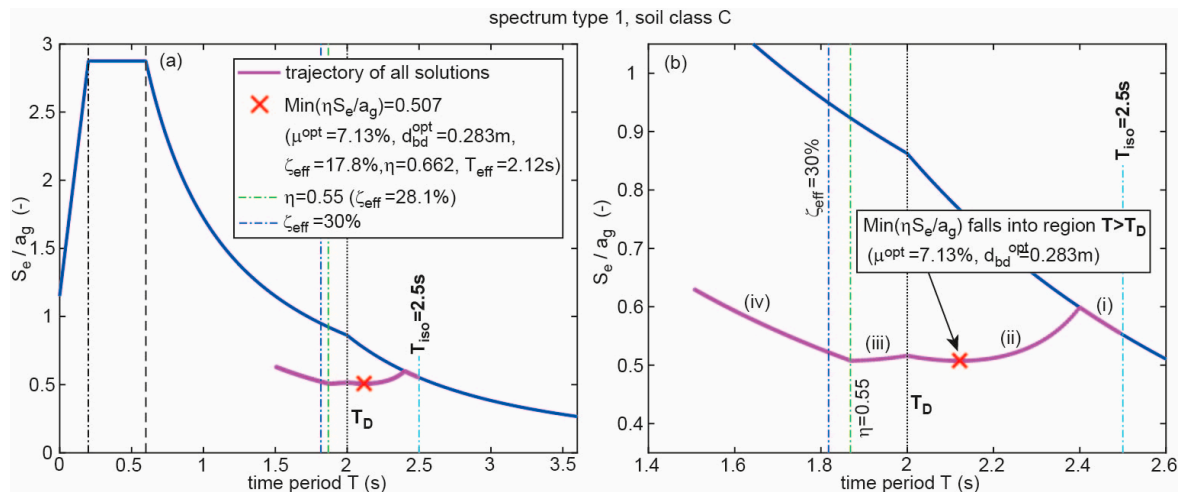


Figure 7. (a) Optimization trajectory for $T_{iso} = 2.5$ s and (b) according close-up for spectrum type 1 with soil class C.

2.3.2. Optimum Solutions as Function of Isolation Time Period

In Section 2.3.1 the optimization trajectories with the according optimum CSS designs are shown for some selected isolation time periods, i.e., $T_{iso} = 1.9$ s, 2.49 s, 2.5 s and 3.5 s. The logical next step is to have a look only at how the optimum CSS design solutions depend on T_{iso} . Figure 8 shows how the optimum design parameters of the CSS, i.e., the optimum friction coefficient μ^{opt} and the optimum displacement capacity d_{bd}^{opt} , and the resulting minimized structural acceleration response depend on T_{iso} . The other state variables of interest of the optimum CSS design solutions, i.e., ζ_{eff} , η , T_{eff} , F_b/N_S , and E_s/E_h , are depicted in Figure 9 as a function of T_{iso} . The following main observation can be made:

- The longer T_{iso} is the smaller the optimum friction coefficient μ^{opt} becomes.
- The displacement capacities d_{bd}^{opt} of all optimum CSS design solutions whose effective time periods lie in the region $T_{eff} > T_D$ are constant because at $T_{eff} > T_D$ the reduction factor $\eta = 0.66$ is constant and $\eta S_e/a_g$ at $T_{eff} > T_D$ is in proportion to $1/T^2$ whereby the according displacement is constant.; notice that $d_{bd}^{opt} = \text{constant}$ at $T_{eff} > T_D$ only applies to the optimum CSS design solutions due to $\eta = \text{constant}$ in this time period range.
- The optimum CSS design in the typical isolation time period region $3.5 \text{ s} < T_{iso} < 4.5 \text{ s}$ is not obtained from maximum tolerated effective damping ratio $\zeta_{eff} = 30\%$ but from the lower value $\zeta_{eff} = 17.8\%$ evoking $\eta = 0.66$.
- The jump in the curves of the shown state variables at $T_{iso} = 2.5$ s is caused by the fact that the optimum CSS design lies in the region $T_{eff} < T_D$ if $T_{iso} < 2.5$ s, while it is located in the region $T_{eff} > T_D$ if $T_{iso} \geq 2.5$ s.
- Reasonable values for F_b/N_S are found in the typical isolation time period region $3.5 \text{ s} < T_{iso} < 4.5 \text{ s}$.
- The re-centring condition $E_s/E_h \geq 0.25$ is fulfilled for all optimum CSS designs and all considered isolation time periods T_{iso} .

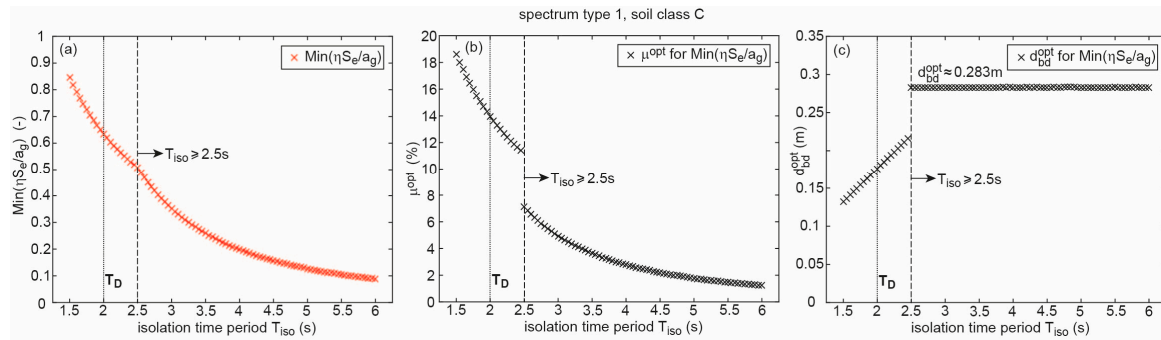


Figure 8. (a) Minimum structural acceleration due to optimum selections of (b) friction coefficient and (c) displacement capacity for spectrum type 1 with soil class C.

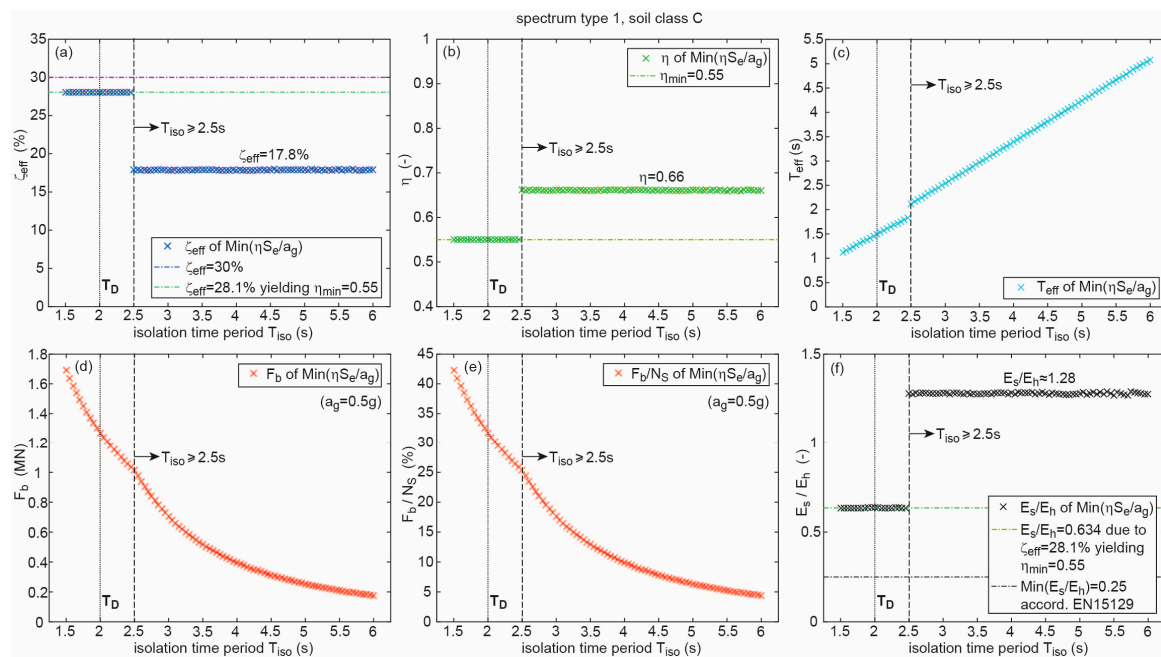


Figure 9. States of optimum solution: (a) effective damping ratio; (b) reduction factor; (c) effective time period; (d,e) maximum horizontal CSS force; (f) re-centring condition for spectrum type 1 with soil class C. N_s : vertical load on CSS; η_{min} : minimum reduction factor.

2.4. Optimization Results for Spectrum of Type 2 with Soil Class C

The optimization trajectories associated by their optimum CSS designs for spectrum of type 2 and soil class C are depicted in Figures 10 and 11. Since $T_D = 1.2$ s for type 2 is much lower than $T_D = 2$ s for type 1 the optimum CSS design solution lies in the region $T_{eff} < T_D$ if $T_{iso} < 1.5$ s and in the region $T_{eff} > T_D$ if $T_{iso} \geq 1.5$ s, which explains the jump in the state variables at $T_{iso} = 1.5$ s (Figures 12 and 13). Similar to the results for spectrum of type 1 not the maximum tolerated effective damping ratio $\zeta_{eff} = 30\%$ with associated $\eta = 0.55$, but $\zeta_{eff} = 17.6\%$ with associated $\eta = 0.66$ minimizes the structural acceleration response. For $T_{iso} < 1.5$ s, the optimum damping ratio also differs from its tolerated maximum because $\zeta_{eff} \approx 28.1\%$ yields the minimum value of η , i.e., $\eta_{min} = 0.55$, whereby any augmentation of ζ_{eff} above 28.1% does not further reduce S_e . Also, the re-centring condition is fulfilled for all considered T_{iso} and shows the same value as for spectrum of type 1.

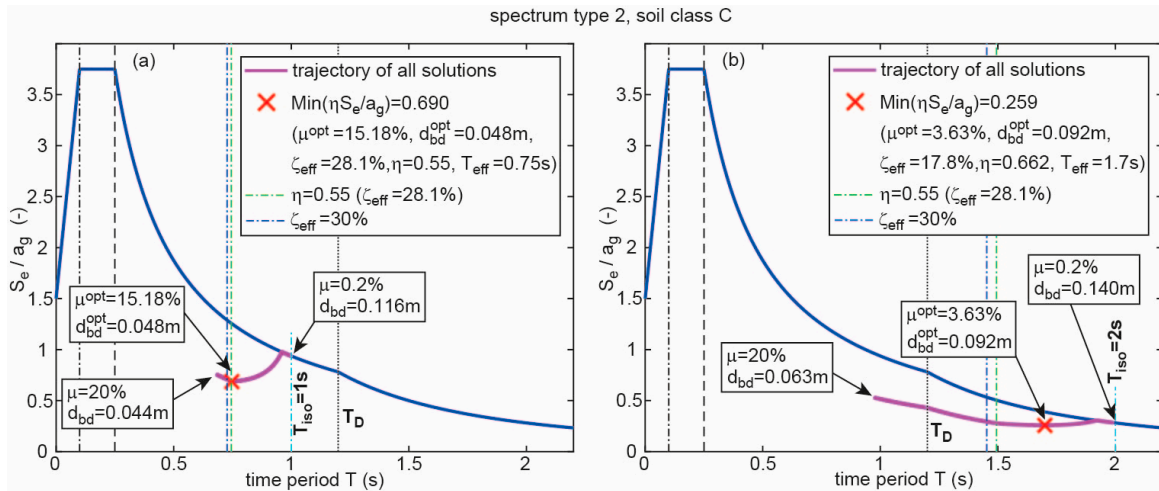


Figure 10. Optimization trajectories for (a) $T_{iso} = 1$ s and (b) $T_{iso} = 2$ s for spectrum type 2 with soil class C.

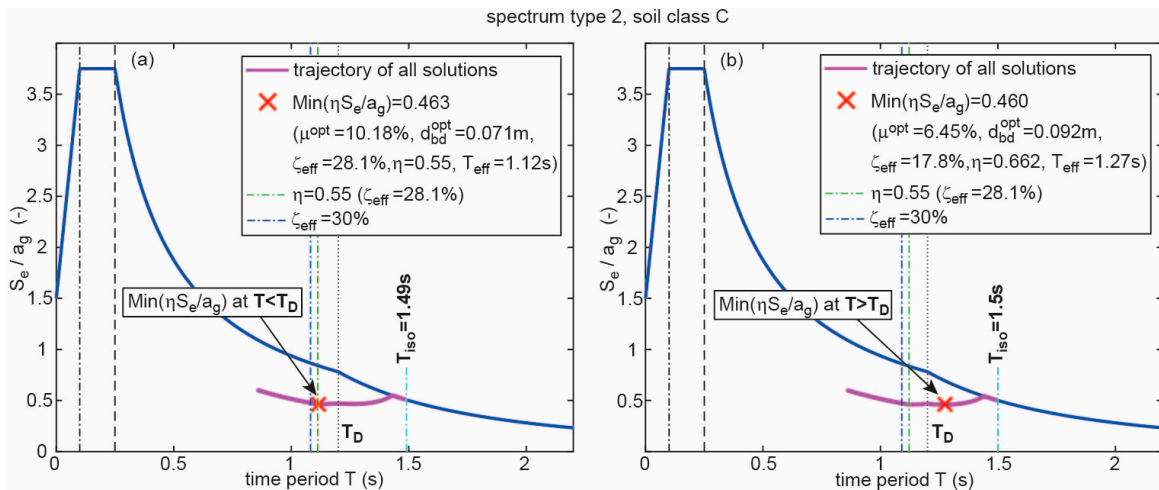


Figure 11. Optimization trajectories for (a) $T_{iso} = 1.49$ s and (b) $T_{iso} = 1.5$ s for spectrum type 2 with soil class C.

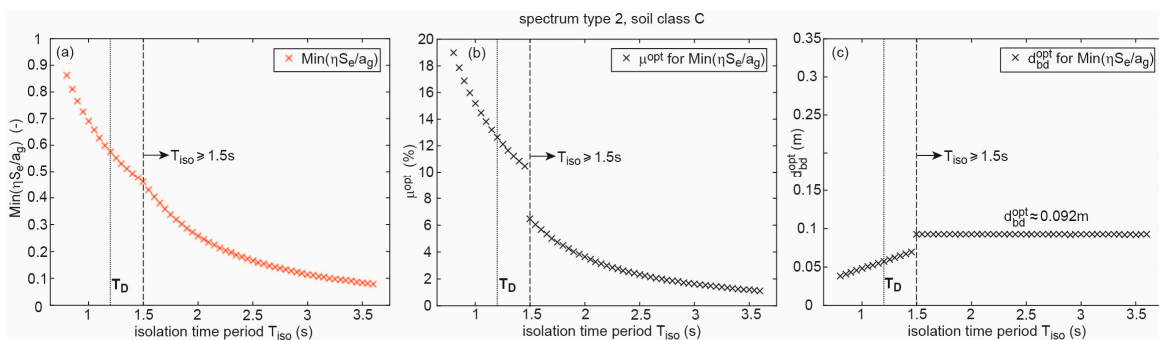


Figure 12. (a) Minimum structural acceleration due to optimum selections of (b) friction coefficient and (c) displacement capacity for spectrum type 2 with soil class C.

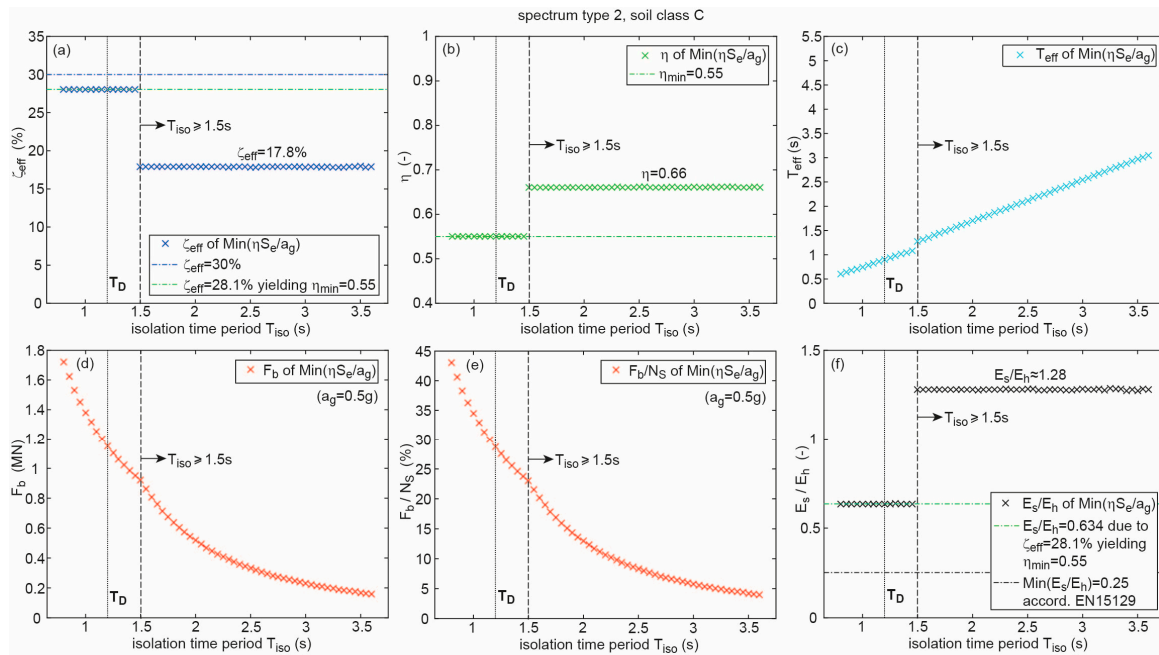


Figure 13. States of optimum solution: (a) effective damping ratio; (b) reduction factor; (c) effective time period; (d,e) maximum horizontal CSS force; (f) re-centring condition for spectrum type 2 with soil class C.

3. Sensitivity of Friction Coefficient on Structural Acceleration

This section describes quantitatively by how much the structural acceleration worsens when the actual friction coefficient of the real CSS deviates from its optimum value minimizing structural acceleration.

3.1. Sensitivity Formulation

The reduced structural acceleration response ηS_e computed as function of friction coefficient μ , as depicted in Figure 14a basically shows by how much the structural acceleration response deteriorates (increases) if the actual friction coefficient of the real CSS deviates (being smaller or greater) from its optimum value μ^{opt} . The sensitivity is defined as the relative change in the system's output (relative change in structural acceleration) for given relative change in the system's input (relative change in friction coefficient). Hence, the sensitivity curve is obtained by, first, subtracting the minimum value from the structural acceleration and the optimum value from the friction coefficient, respectively, and, subsequently, normalizing the first term by its minimum value, and the second term by its optimum value (Figure 14b)

$$sensitivity = \frac{\{\eta S_e - Min(\eta S_e)\} / Min(\eta S_e)}{\{\mu - \mu^{opt}\} / \mu^{opt}} = \frac{\delta S_e / S_e^{opt}}{\delta \mu / \mu^{opt}} \quad (8)$$

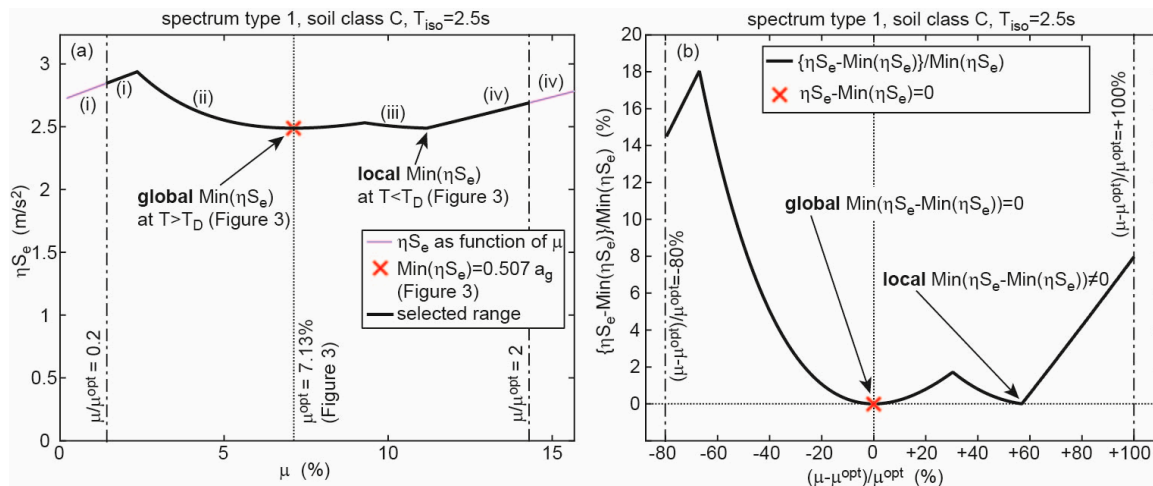


Figure 14. Derivation of sensitivity curves (shown for spectrum type 1 with soil class C and $T_{iso} = 2.5$ s): (a) reduced acceleration response ηS_e as function of friction coefficient μ and (b) according sensitivity curve.

Please note that this sensitivity analysis does not investigate the impact of deviations in μ on the resulting displacement capacity. It is common understanding that a lower actual friction coefficient of the real CSS than its design value will cause larger relative motions in the CSS, as, e.g., visible in Figures 4b and 5b.

3.2. Results for Spectrum of Type 1

The sensitivity curves for spectrum of type 1 with soil class C are depicted in Figures 15–17 for the selected isolation time periods $T_{iso} = 2$ s, 2.5 s, 3 s, 3.5 s, 4 s and 4.5 s. The sensitivity curves for the unusually low $T_{iso} = 2$ s and 2.5 s are also plotted to demonstrate that structural acceleration is more sensitive to deviations in the actual friction coefficient if T_{iso} is unusually low (2 s) and that structural acceleration does hardly deteriorate for $\mu - \mu^{opt} > 0$ if $T_{iso} = 2.5$ s due to the special case that the global and local minima yield a fairly flat sensitivity curve at $\mu - \mu^{opt} > 0$. Horizontal dash-dotted lines in different colours corresponding to different levels of deterioration in $\delta S_e / S_e^{opt}$ are included in Figures 15–17 to be able to directly read off by how much the actual friction coefficient may deviate (plus and minus) from its optimum value if a certain level of acceptable deterioration in structural acceleration is assumed. For instance, the structural engineer may estimate that the structural acceleration may deteriorate by +5% (green dash-dotted line) and then read off directly from the sensitivity curves by how much the actual friction coefficient of the real CSS may differ from its optimum value. For the assumption that $\delta S_e / S_e^{opt} = +5\%$ may be acceptable the sensitivity curves with reasonable isolation time periods $T_{iso} = 3$ s to 4.5 s demonstrate that the actual friction coefficient of the real CSS may deviate from its optimum value by at least $\delta \mu / \mu^{opt} = -39.7\%$ and +55.6%. The tolerances are not symmetric relative to μ^{opt} because of the non-symmetrical sensitivity curves.

Sensitivity curves are also computed for spectrum of type 1 with soil classes A, B, D, and E. The results of these computations are evaluated for acceptable deteriorations in $\delta S_e / S_e^{opt}$ of +5% and +2% and summarized in Table 1, together with the results for spectrum of type 1 with soil class C. This table reveals that—for reasonable isolation time periods $3 \text{ s} \leq T_{iso} \leq 4.5 \text{ s}$ (in grey) for spectrum of type 1—the actual friction coefficient of the real CSS may differ from its optimum value by at least (minimum tolerated deviations, bold style) $\delta \mu / \mu^{opt} = -39.5\%$ and +54.5% if $\delta S_e / S_e^{opt} = +5\%$ may be acceptable, and by at least (minimum tolerated deviations, bold style) $\delta \mu / \mu^{opt} = -26.2\%$ and +32.0% if $\delta S_e / S_e^{opt} = +2\%$ is considered to be acceptable.

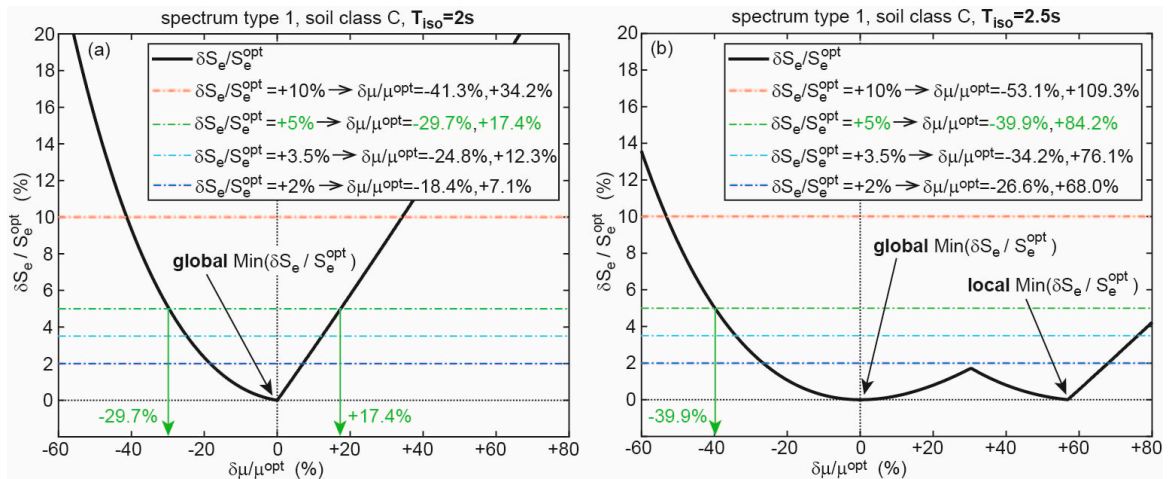


Figure 15. Sensitivity of deviation in friction coefficient from its optimum value on relative increase of structural acceleration for (a) $T_{iso} = 2s$ and (b) $T_{iso} = 2.5s$ and spectrum of type 1 with soil class C. $\delta S_e / S_e^{opt}$: deviation of structural acceleration relative to its optimum (minimum) value; $\delta \mu / \mu^{opt}$: deviation of friction coefficient relative to its optimum value.

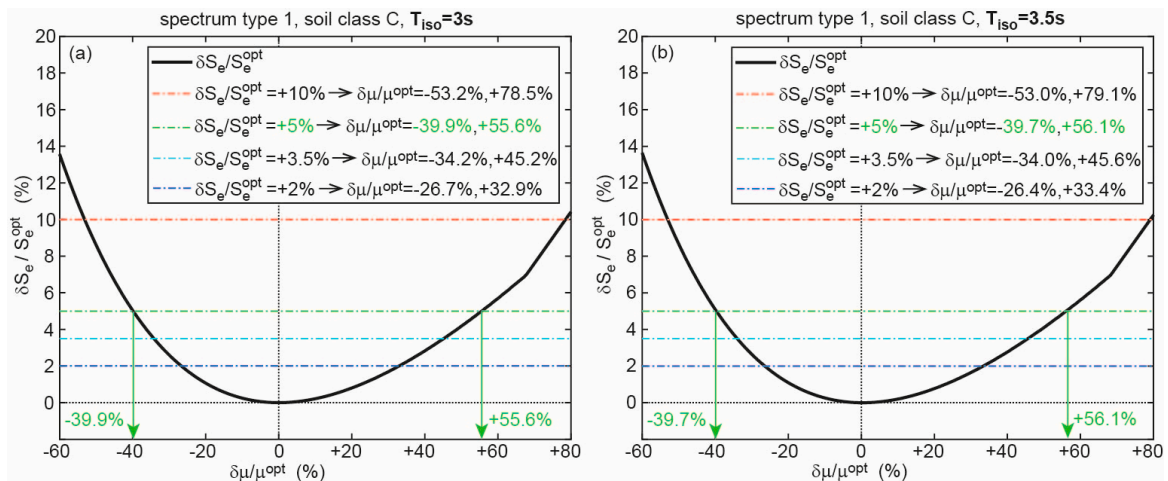


Figure 16. Sensitivity of deviation in friction coefficient from its optimum value on relative increase of structural acceleration for (a) $T_{iso} = 3s$ and (b) $T_{iso} = 3.5s$ and spectrum of type 1 with soil class C.

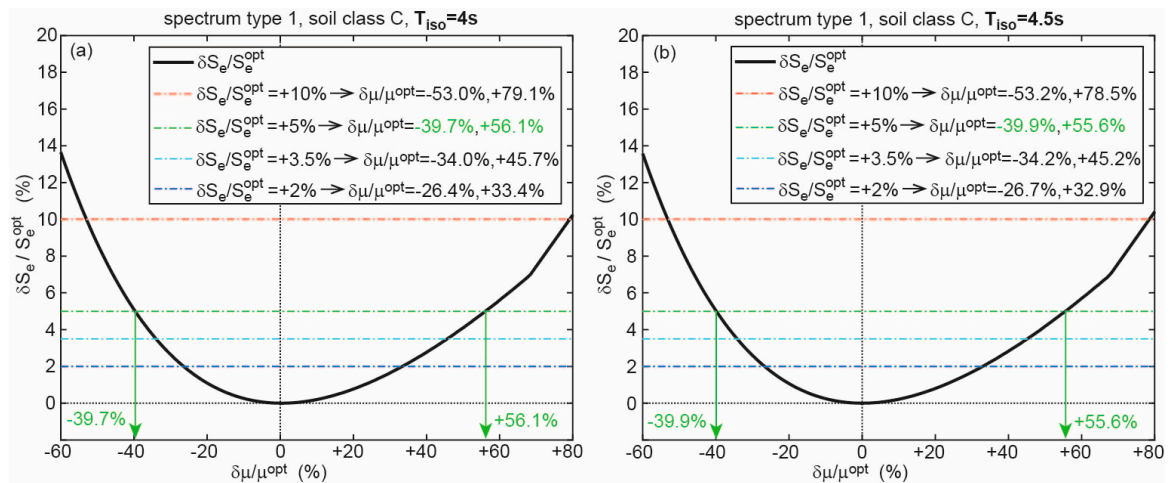


Figure 17. Sensitivity of deviation in friction coefficient from its optimum value on relative increase of structural acceleration for (a) $T_{iso} = 4$ s and (b) $T_{iso} = 4.5$ s and spectrum of type 1 with soil class C.

Table 1. Sensitivity results for spectrum of type 1 for relative increase of +5% and +2% in structural acceleration.

T_{iso} (s)	Soil Class	$ffiS_e/S_e^{opt}$	$ffi^-/-opt$	$ffiS_e/S_e^{opt}$	$ffi^-/-opt$
2	A	+5%	-29.6%, +17.7%	2%	-18.3%, +7.3%
	B	+5%	-29.7%, +17.4%	2%	-18.4%, +7.0%
	C	+5%	-29.7%, +17.4%	2%	-18.4%, +7.1%
	D	+5%	-29.6%, +17.5%	2%	-18.3%, +7.1%
	E	+5%	-29.6%, +17.6%	2%	-18.3%, +7.2%
2.5	A	+5%	-39.8%, +84.4%	2%	-26.6%, +68.1%
	B	+5%	-39.9%, +84.0%	2%	-26.7%, +67.8%
	C	+5%	-39.9%, +84.2%	2%	-26.6%, +68.0%
	D	+5%	-39.9%, +84.1%	2%	-26.7%, +67.9%
	E	+5%	-39.9%, +84.2%	2%	-26.7%, +67.9%
3	A	+5%	-40.0%, +55.2%	2%	-26.9%, +32.7%
	B	+5%	-39.8%, +55.7%	2%	-26.6%, +33.0%
	C	+5%	-39.9%, +55.6%	2%	-26.7%, +32.9%
	D	+5%	-39.9%, +55.5%	2%	-26.7%, +32.8%
	E	+5%	-40.0%, +55.4%	2%	-26.8%, +32.8%
3.5	A	+5%	-39.7%, +56.2%	2%	-26.4%, +33.4%
	B	+5%	-39.7%, +56.1%	2%	-26.4%, +33.4%
	C	+5%	-39.7%, +56.1%	2%	-26.4%, +33.4%
	D	+5%	-40.0%, +55.3%	2%	-26.8%, +32.7%
	E	+5%	-40.1%, +55.1%	2%	-26.9%, +32.5%
4	A	+5%	-40.3%, +54.5%	2%	-27.2%, +32.0%
	B	+5%	-40.0%, +55.2%	2%	-26.8%, +32.7%
	C	+5%	-39.7%, +56.1%	2%	-26.4%, +33.4%
	D	+5%	-39.8%, +55.8%	2%	-26.6%, +33.1%
	E	+5%	-39.9%, +55.5%	2%	-26.7%, +32.8%
4.5	A	+5%	-39.9%, +55.6%	2%	-26.6%, +32.9%
	B	+5%	-39.5%, +56.6%	2%	-26.2%, +33.8%
	C	+5%	-39.9%, +55.6%	2%	-26.7%, +32.9%
	D	+5%	-40.0%, +55.2%	2%	-26.8%, +32.6%
	E	+5%	-39.7%, +56.0%	2%	-26.5%, +33.3%

Table 1. Cont.

T_{iso} (s)	Soil Class	$ffiS_e/S_e^{opt}$	$ffi^-/-opt$	$ffiS_e/S_e^{opt}$	$ffi^-/-opt$
5	A	+5%	-39.4% , +56.7%	2%	-26.1%, +33.9%
	B	+5%	-39.9% , +55.4%	2%	-26.7%, +32.8%
	C	+5%	-39.7% , +56.1%	2%	-26.4%, +33.4%
	D	+5%	-40.2% , +54.9%	2%	-27.0%, +32.3%
	E	+5%	-39.6% , +56.2%	2%	-26.4%, +33.4%

Values in bold type represent the minimum tolerated deviations in the friction coefficient for reasonable (shaded) isolation time periods.

3.3. Results for Spectrum of Type 2

Analogue to the results for spectrum of type 1 the sensitivity curves for spectrum of type 2 with soil class C are graphically presented (Figures 18–20) and all sensitivities resulting from spectrum of type 2 with all the soil classes evaluated at $\delta S_e/S_e^{opt} = +5\%$ and $+2\%$ are summarized in Table 2. For reasonable $1.8\text{ s} \leq T_{iso} \leq 2.7\text{ s}$ (in grey), it is seen that the actual friction coefficient of the real CSS may differ from its optimum value by at least (minimum tolerated deviations, bold style) $\delta\mu/\mu^{opt} = -39.7\%$ and $+54.9\%$ assuming $\delta S_e/S_e^{opt} = +5\%$ is acceptable and by at least (minimum tolerated deviations, bold style) $\delta\mu/\mu^{opt} = -26.4\%$ and $+32.4\%$ if $\delta S_e/S_e^{opt} = +2\%$ is assumed to be acceptable. These results are very similar to those for spectrum of type 1 because the relative deterioration of the structural acceleration depends on the relative change of the friction coefficient.

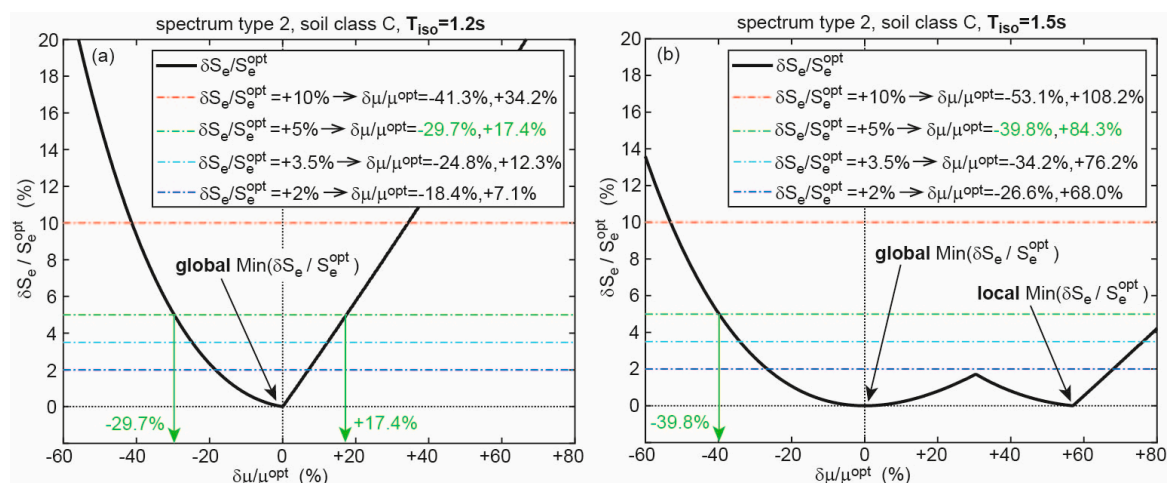


Figure 18. Sensitivity of deviation in friction coefficient from its optimum value on relative increase of structural acceleration for (a) $T_{iso} = 1.2\text{ s}$ and (b) $T_{iso} = 1.5\text{ s}$ and spectrum of type 2 with soil class C.

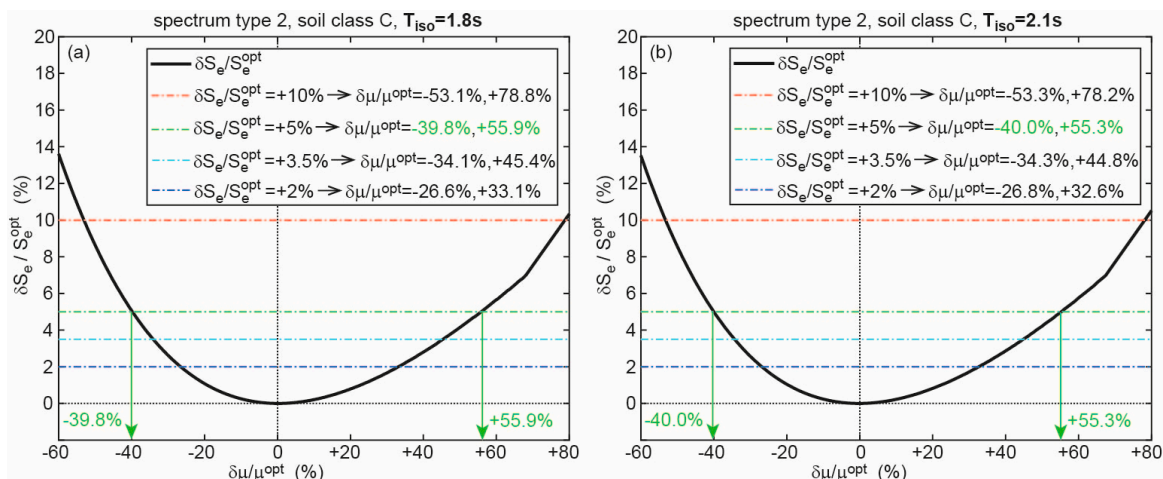


Figure 19. Sensitivity of deviation in friction coefficient from its optimum value on relative increase of structural acceleration for (a) $T_{iso} = 1.8$ s and (b) $T_{iso} = 2.1$ s and spectrum of type 2 with soil class C.

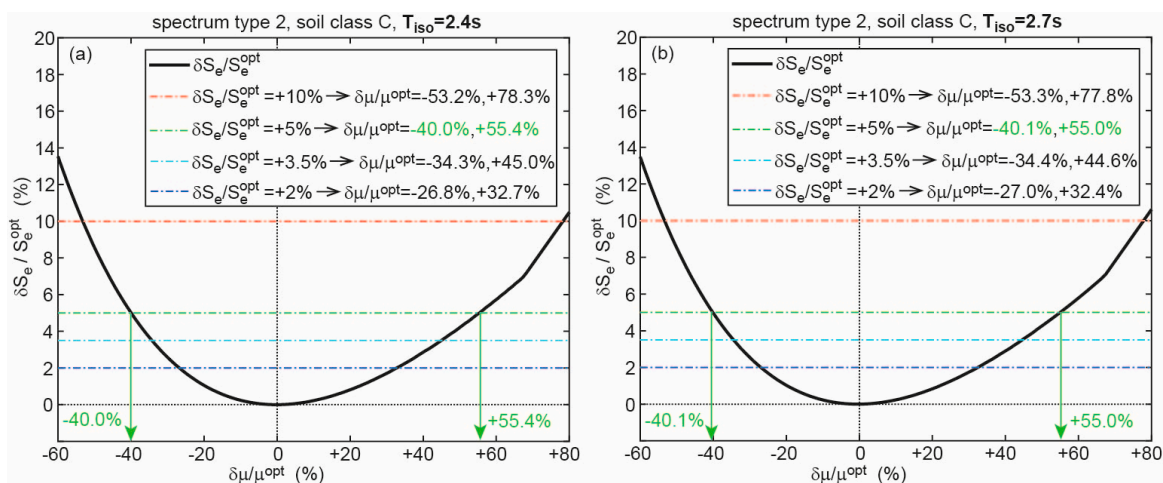


Figure 20. Sensitivity of deviation in friction coefficient from its optimum value on relative increase of structural acceleration for (a) $T_{iso} = 2.4$ s and (b) $T_{iso} = 2.7$ s and spectrum of type 2 with soil class C.

Table 2. Sensitivity results for spectrum of type 2 for relative increase of +5% and +2% in structural acceleration.

T_{iso} (s)	Soil Class	$ffiS_e/S_e^{opt}$	$ffi^{-}/-^{opt}$	$ffiS_e/S_e^{opt}$	$ffi^{-}/-^{opt}$
1.2	A	+5%	−29.7%, +17.6%	2%	−18.3%, +7.1%
	B	+5%	−29.7%, +17.5%	2%	−18.4%, +7.1%
	C	+5%	−29.7%, +17.4%	2%	−18.4%, +7.1%
	D	+5%	−29.6%, +17.6%	2%	−18.3%, +7.2%
	E	+5%	−29.7%, +17.4%	2%	−18.4%, +7.1%
1.5	A	+5%	−39.9%, +84.1%	2%	−26.7%, +67.9%
	B	+5%	−39.8%, +84.4%	2%	−26.6%, +68.2%
	C	+5%	−39.8%, +84.3%	2%	−26.6%, +68.0%
	D	+5%	−39.9%, +84.0%	2%	−26.7%, +67.8%
	E	+5%	−39.8%, +84.3%	2%	−26.6%, +68.1%

Table 2. Cont.

T_{iso} (s)	Soil Class	$ffiS_e/S_e^{opt}$	$ffi^- / -opt$	$ffiS_e/S_e^{opt}$	$ffi^- / -opt$
1.8	A	+5%	−39.7%, +56.2%	2%	−26.4%, +33.5%
	B	+5%	−39.7%, +55.9%	2%	−26.5%, +33.2%
	C	+5%	−39.8%, +55.9%	2%	−26.6%, +33.1%
	D	+5%	−39.9%, +55.6%	2%	−26.6%, +33.0%
	E	+5%	−39.8%, +55.8%	2%	−26.6%, +33.1%
2.1	A	+5%	−40.0%, +55.2%	2%	−26.9%, +32.5%
	B	+5%	−40.1%, +55.0%	2%	−27.0%, +32.4%
	C	+5%	−40.0%, +55.3%	2%	−26.8%, +32.6%
	D	+5%	−40.0%, +55.3%	2%	−26.8%, +32.7%
	E	+5%	−39.7%, +56.2%	2%	−26.4%, +33.4%
2.4	A	+5%	−39.7%, +56.0%	2%	−26.5%, +33.3%
	B	+5%	−40.0%, +55.2%	2%	−26.8%, +32.6%
	C	+5%	−40.0%, +55.4%	2%	−26.8%, +32.7%
	D	+5%	−39.8%, +55.8%	2%	−26.6%, +33.1%
	E	+5%	−40.1%, +55.0%	2%	−27.0%, +32.4%
2.7	A	+5%	−39.8%, +55.7%	2%	−26.6%, +33.1%
	B	+5%	−40.1%, +54.9%	2%	−27.0%, +32.4%
	C	+5%	−40.1%, +55.0%	2%	−27.0%, +32.4%
	D	+5%	−40.0%, +55.2%	2%	−26.9%, +32.6%
	E	+5%	−39.9%, +55.6%	2%	−26.7%, +32.9%
3	A	+5%	−39.9%, +55.6%	2%	−26.6%, +32.9%
	B	+5%	−39.8%, +55.8%	2%	−26.5%, +33.2%
	C	+5%	−40.3%, +54.5%	2%	−27.2%, +32.0%
	D	+5%	−39.9%, +55.5%	2%	−26.7%, +32.8%
	E	+5%	−40.0%, +55.3%	2%	−26.8%, +32.7%

Values in bold type represent the minimum tolerated deviations in the friction coefficient for reasonable (shaded) isolation time periods.

4. Summary and Conclusions

This paper first presents an optimization routine that derives all the valid designs of CSS based on the method of the linear response spectrum. All of the valid CSS designs are represented by their acceleration trajectory in the elastic response spectrum plane. The fairly flat minimum of the acceleration trajectory reveals that deviations in the actual friction coefficient of the real CSS from its optimum value do not have great deteriorating impact on structural acceleration.

The second part of this study describes how friction coefficient, displacement capacity, effective damping ratio, reduction factor, effective time period, and re-centring condition of all optimum CSS solutions for minimum structural acceleration depend on isolation time period. The results for reasonable isolation time periods demonstrate that the optimum CSS, which minimizes structural acceleration, is not obtained at maximum tolerated effective damping ratio of 30% of the CSS, but at a significantly lower value.

The third and final part of the paper is concerned with the question by how much the structural acceleration deteriorates when the actual friction coefficient of the real CSS differs from its optimum value. The underlying sensitivity analysis, which is performed for spectra of type 1 and 2 and all soil classes, demonstrates that the relative increase in the structural acceleration is approximately one order of magnitude smaller than the assumed deviation in the actual friction coefficient from its optimum value. The sensitivity results may be used by the structural engineer to define tolerable deviations in the actual friction coefficient from its optimum value, such that the resulting structural acceleration response is still acceptably small.

Acknowledgments: The authors gratefully acknowledge the financial supports of Maurer Switzerland GmbH, Zurich, Switzerland, MAURER ENGINEERING GmbH, Munich, Germany, and MAURER SE, Munich, Germany.

Author Contributions: Felix Weber, Leopold Meier and Johann Distl performed the optimization analysis; Felix Weber and Christian Braun made the sensitivity analysis; all authors were involved in writing the paper.

Conflicts of Interest: The authors declare no conflict of interest.

References

1. Yen, K.Z.Y.; Lee, Y.J. Passive Vibration Isolating System. U.S. Patent No. 6126136, 3 October 2000.
2. European Committee for Standardization. *Eurocode 8: Design of Structures for Earthquake Resistance—Part 1: General Rules, Seismic Actions and Rules for Buildings*; EU: Brussels, Belgium, 2004; 321p.
3. Lai, M.L.; Soong, T.T. Seismic design considerations for secondary structural systems. *J. Struct. Eng.* **1991**, *117*, 459–472. [[CrossRef](#)]
4. Inaudi, J.A.; Kelly, J.M. Optimum damping in linear isolation systems. *Earthq. Eng. Struct. Dyn.* **1993**, *22*, 583–598. [[CrossRef](#)]
5. Kelly, J.M. The role of damping in seismic isolation. *Earthq. Eng. Struct. Dyn.* **1999**, *28*, 3–20. [[CrossRef](#)]
6. Hall, J.F. Discussion: The role of damping in seismic isolation. *Earthq. Eng. Struct. Dyn.* **1999**, *28*, 1717–1720. [[CrossRef](#)]
7. Du, Y.; Zhao, G. Analysis of effect of non-classical damping on isolated structure and optimum damping. *J. Earthq. Eng. Eng. Vib.* **2000**, *20*, 100–107.
8. Jangid, R.S. Optimum friction pendulum system for near-fault motions. *Eng. Struct.* **2005**, *27*, 349–359. [[CrossRef](#)]
9. Bucher, C. Probability-based optimization of friction damping devices. *Struct. Saf.* **2009**, *31*, 500–507. [[CrossRef](#)]
10. Kovaleva, N.V.; Rutman, Y.L.; Davydova, G.V. Determination of optimal damping parameters for seismic isolation systems. *Mag. Civ. Eng.* **2013**, *40*, 107–115. [[CrossRef](#)]
11. Nigdeli, S.M.; Bekdaş, G.; Alhan, C. Optimization of seismic isolation systems via harmony search. *Eng. Optim.* **2014**, *46*, 1553–1569. [[CrossRef](#)]
12. Kamalzare, M.; Johnson, E.A.; Wojtkiewicz, S.F. Efficient optimal design of passive structural control applied to isolator design. *Smart Struct. Syst.* **2015**, *15*, 847–862. [[CrossRef](#)]
13. Mazza, F. Lateral-torsional response of base-isolated buildings with curved surface sliding system subjected to near-fault earthquakes. *Mech. Syst. Signal Process.* **2017**, *92*, 64–85. [[CrossRef](#)]
14. Mazza, F.; Mazza, M. Sensitivity to modelling and design of curved surface sliding bearings in the nonlinear seismic analysis of base-isolated r.c. framed buildings. *Soil Dyn. Earthq. Eng.* **2017**, *79*, 951–970. [[CrossRef](#)]



© 2018 by the authors. Licensee MDPI, Basel, Switzerland. This article is an open access article distributed under the terms and conditions of the Creative Commons Attribution (CC BY) license (<http://creativecommons.org/licenses/by/4.0/>).